Asian Journal of Chemistry; Vol. 26, No. 18 (2014), 6101-6105

ASIAN JOURNAL OF CHEMISTRY

http://dx.doi.org/10.14233/ajchem.2014.16780

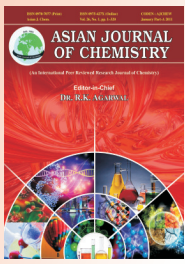

Effect of Calcination Temperature in Preparation of ZnO-SiO_2/Laponite and its Physical Character and Photocatalytic Activity

IS FATIMAH

Chemistry Department, Islamic University of Indonesia, Kampus Terpadu UII.Jl. Kaliurang Km 14, Yogyakarta, Indonesia

Corresponding author: E-mail: isfatimah@uii.ac.id

Received: 28 November 2013; *Accepted*: 12 February 2014; *Published online*: 1 September 2014; AJC-15862

ZnO-SiO_2/laponite was prepared by sol-gel preparation procedure consit of SiO_2 pillarization to laponite followed by ZnO dispersion by using zinc acetate as precursor. The obtained material was characterized by X-ray diffraction, scanning electron microscopy, energy dispersive spectrometry, diffuse reflectance UV-visible (DRUV-visible) and N_2 adsorption-desorption analysis. The photocatalytic performance of the material in decolorization of methylene blue was also investigated. Compared with ZnO-SiO_2 nanoparticles, it is concluded that ZnO-SiO_2/laponite possess higher photocatalytic activity and influenced by calcination temperature.

Keywords: Clay, Photocatalyst, Pillarization, ZnO-SiO_2, Laponite.

INTRODUCTION

Photocatalysis and photooxidation over semiconductor photocatalys has been growing technology in recent years. Beside the use of TiO_2, some researchers pay attention on ZnO utilization and its photocatalytic enhancement *via* composite formation by using some silica or silica alumina materials. Zinc oxide (ZnO) has direct bandgap of 3.37 eV and from some studies, it is evaluated as high activity, low cost and environmentally friendly feature[1-5]. By dispersing onto a solid support, photocatalytic activity can be enhanced by limiting the recombination of electrone-hole during the photocatalysis mechanism. For this purposes, the insertion of ZnO particles into a layer structure of clay is an interesting topic. In spite of direct insertion of ZnO nanoparticles into interlayer space of clay; another method can be attempted to get a stable and homogeneous ZnO is dispersion onto pillared clay. One of the methods is sol-gel process to prepare ZnO embedded SiO_2 which is relatively easy to formed. With its easy and simple prepared porous structure to enhance photoactivity and homogeneous distribution of ZnO, preparation of ZnO-SiO_2 are intensely studied[6-9]. Furthermore, for environmental photocatalytic application, highly surface area and porous structure of material are required. To overcome the limitation of activity reduction as used, this study deals with preparation of ZnO-SiO_2 in composite form with laponite clay. By adopting pillarization process, ZnO-SiO_2 was inserted into interlayer of laponite clay structure and based on its thermal stability and porosity, ZnO-SiO_2 can be distributed homogeneously on surface. Considering that physicochemical properties of material affects the photocatalytic activity, study on preparation, characterization and photo-catalytic activity test of ZnO-SiO_2 immobilized laponite clay was interesting topic conducted in this investigation. A preparation variable of calcination temperature was hypothesized affecting nanoparticle size of ZnO-SiO_2, distribution and photoactivity enhancement to ZnO-SiO_2 in the composite formation. The aim of this study was to evaluate the relationshop between physicochemical character and photocatalytic behaviour of materials derived by different variables. Material character was evaluated by surface parameter, material crystallinity, surface morphology and band gap energy while for photocatalytic activity, kinetics study on photocatalysis and photooxidation of methylene blue over prepared material was simulated.

EXPERIMENTAL

Tetraethyl orthosilicate (TEOS) was purchased from Merck-Millipore, zinc acetate dihydrate, cetyltrimethyl ammonium bromide and nitric acid and phospate buffer were obtained from Merck-Milipore and laponite (LAP) clay obtained from southern clay product, Inc.

ZnO-SiO_2/laponite (furthermore called as ZnO-SiO_2/LAP) preparation was conducted in two steps of synthesis *i.e.*, preparation of SiO_2-laponite sol and ZnO-SiO_2/laponite. For SiO_2-laponite sol preparation, firstly surfactant of cetyltrimethyl ammonium bromide solution in ethanol was added slowly into the homogeneous solution of 1 % w/v laponite solution in

water was made with final proportion of cetyltrimethyl ammonium bromide to laponite of 50 mmol/100 g. Tetraethyl orthosilicate as silica precursor was then added drop wise into the suspension followed by stirring for 24 h until the composition of Si to laponite of 10 mmol/100 g reached. The sol was then aged at 40 °C for 6 days before then mix with Zn-acetate solution in ethanol with stirring for 4 h. The prepared sol was also white transparent at room temperature and kept for 24 h. Filtrate of ZnO-SiO_2/laponite gel was obtained by filtering the mixture and the filtrate was dried at 40 °C before calcination at varied temperature of 400, 500, 600 and 700 °C. The heat treatment procedures were applied with a heating rate of 5 °C/min up to targeted temperature under an air atmosphere and cooled over night inside the furnace. Samples obtained by these varied procedure were then designated as ZnO-SiO_2/LAP-400 to ZnO-SiO_2/LAP-700 regarding to calcination temperature. As a standard, ZnO-SiO_2 was produced by similar sol-gel method. Zn precursor was prepared by diluting Zn-acetate dihydrate in ethanol and then added drop wise into TEOS in ethanol under vigorous stirring for 24 h. Mol ratio of Zn: Si was setted up to 3:7. The transparent sol was further dried and aged at 40 °C for 6 days until white gel was obtained after calcination at 500 °C.

Phase identification and crystallite size of samples were characterized using a Philips PW1800 X-ray diffractometer with nickel-filtered CuK_α radiation (λ = 1.5406 Å) at 40 kV and 30 mA. The Debye-Scherrer formula (Eqn. 1) was applied to measure the crystallite size of ZnO in each sample. The surface morphology and spot analysis of samples were examined by a SEM-EDX Seiko and the BET surface area and the pore size distribution of the calcined nanopowders were determined by a BET surface area analyzer (NOVA 1200) using N_2 as the adsorptive gas. Diffuse reflectance UV-visible absorption spectra were recorded on a Shimadzu J6000 UV-visible spectrometer equipped with a Diffuse Reflectance cell. Photocatalytic property of the samples was tested in methylene blue degradation by photocatalysis and photooxidation mechanism. Pyrex glass reactor with stirrer placed 20 cm under UV A Lamp as artificial light in a closed box system was used for photocatalytic testing. Sample powder in mixture with methylene blue solution was stirred for certain sampling times. For photooxidation scheme, H_2O_2 of 0.5 % v/v was added as an oxidant. Methylene blue concentration depletion at time of treatment was determined by using spectrophotometric/colorimetric analysis at maximum wavelength of 635.5 nm. For evaluation, initial rate and kinetic constant rate of each reaction was examined during 15 min which determined as reaction reach equillibrium state. For further identification, analysis of treated solution was conducted by high performance liquid chromatography(HPLC) and chemical oxigen demand determination Reusable properties of photocatalyst samples was evaluated by measuring specific surface area and photocatalytic activity of used samples.

RESULTS AND DISCUSSION

Elemental analysis of ZnO-SiO_2/LAP at varied temperature and and ZnO-SiO_2 photocatalysts obtained from gravimetric and EDX analysis are listed in Table-1.

Prepared ZnO-SiO_2 materials showed that Zn content are about 5.3-5.8 % wt. which fit to the theoretical ratio during preparation and the major components are silica and magnesia from the basic structure of laponite as raw material. This is due to main structure of laponite which consists of tetrahedral silica and octahedral magnesia. Another cations of sodium and potasium present as exchangeable native cations between laponite silicate layers to balance the negative charge of main framework of clay structure. N_2 adsorption-desorption and BET isotherm analysis expressed the change in higher adsorbtivity of ZnO-SiO_2/LAP compared to raw laponite material represented from higher values of specific surface area and pore volume parameter (Fig. 1, Table-2). It is also found that

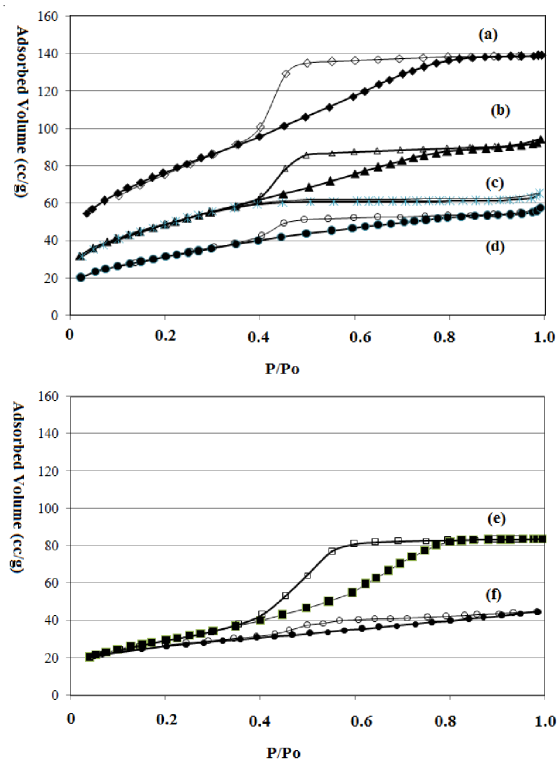

Fig. 1. Adsorption-desorption profile of (a) ZnO-SiO_2/LAP-600 (b) ZnO-SiO_2/LAP-500 (c) ZnO-SiO_2/LAP-400 (d) ZnO-SiO_2/LAP-700 (e) ZnO-SiO_2 (f) Laponite

TABLE-1
ELEMENTAL ANALYSIS OF ZnO-SiO_2/LAP, ZnO-SiO_2 PHOTOCATALYSTS COMPARED TO LAPONITE

No.	Component (% wt.)	ZnO-SiO_2/ LAP-400	ZnO-SiO_2/ LAP-500	ZnO-SiO_2/ LAP-600	ZnO-SiO_2/ LAP-700	ZnO-SiO_2	LAP
1.	Zn	5.81	5.31	5.76	5.32	24.7 %wt.	ud
2.	Si	22.43	23.15	22.12	20.15	21.1 %wt.	59.20
3.	Mg	9.51	15.08	10,23	26.66	ud	27.43
4.	K	0.83	0.8 %wt.	0.75	0.67	ud	ud
5.	Na	0.42	0.43 %wt.	0.33	0.25	ud	2.8

temperature does not affect much to the adsorption-desorption profile even the value of specific surface area and pore volume were significantly affected. The highest specific surface area was gained by ZnO-SiO_2/LAP-600 and from the higher specific surface area of ZnO-SiO_2/LAP calcined at 400-600 °C compared to laponite and the lower value compared to bulk ZnO-SiO_2 indicated the formation of metal oxide pillar in the intercalated space.

TABLE-2
SPECIFIC SURFACE AREA AND PORE VOLUME OF ZnO-SIO_2/LAP AND ZNO-SIO_2 PHOTOCATALYSTS COMPARED TO LAPONITE

No.	Component	Specific surface area(m^2/g)	Pore volume (10^{-3} cc/g)
1.	ZnO-SiO_2/LAP-400	99.55	11.74
2.	ZnO-SiO_2/LAP-500	106.55	36.45
3.	ZnO-SiO_2/LAP-600	229.37	41.14
4.	ZnO-SiO_2/LAP-700	36.69	0.185
5.	ZnO-SiO_2	502.33	48.99
6.	Laponite	99.8	7.93

Thermal effect to the ZnO-SiO_2 formation is revealed by XRD analysis with diffractogram depicted in Fig. 2.

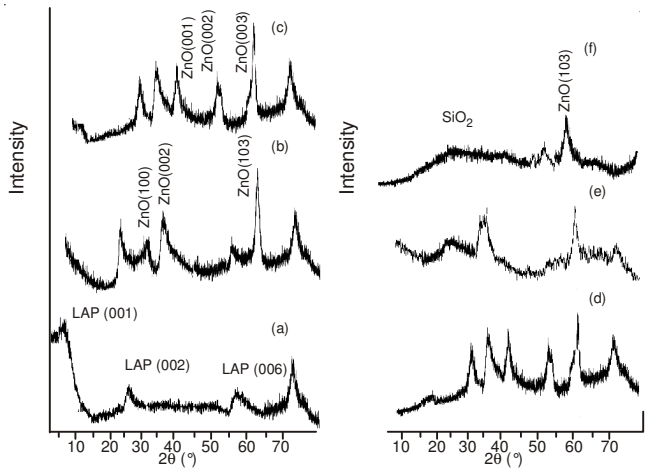

Fig. 2. XRD pattern of (a) LAP (b) ZnO-SiO_2/LAP-400 (c) ZnO-SiO_2/LAP-500 (d) ZnO-SiO_2/LAP-600 (e) ZnO-SiO_2/LAP-700 (f) ZnO-SiO_2

Surface morphology of ZnO-SiO_2/LAP-700 and ZnO-SiO_2/LAP-600 in comparison with ZnO-SiO_2 are also confirmed the change of surface profile as result of thermal effect in that ZnO-SiO_2/LAP-600 look similar surface roughness with ZnO-SiO_2 while ZnO-SiO_2/LAP-700 has different pattern (Fig. 3). Compared to ZnO-SiO_2, ZnO-SiO_2/LAP shows a characteristic peak as indication for ZnO. Both ZnO-SiO_2 and ZnO-SiO_2/LAP exhibit a strong peak at 34.538° correspond to the (002) peaks of ZnO but aother peaks assigned to the present of SiO_2 are not showed. This is probably due to the insertion of SiO_2 homogeneously in laponite as inorganic matrix[6,10].

XRD pattern of materials showed the formation of ZnO-SiO_2 particles in laponite matrix are stable until the calcination temperature of 600 °C. Laponite as support showed the (001); (002) and (006) reflections that are fit to the JCPDS standard and from the (001) reflection it can be found that basal spacing 001 of laponite structure is 14.56. After ZnO-SiO_2 immobilization, some new reflections *i.e* (100); (002) and (103) reflections of ZnO assigned to the presence of ZnO nanoparticles in laponite support. By comparing (002) peak of ZnO, thermal effect on the formation of ZnO crystalline was indicated by the higher crystallinity of ZnO at higher temperature. XRD pattern of varied calcination temperature samples from 400 to 600 °C indicated that the higher calcination temperature affect the particle size of ZnO created as expressed by the tighter ZnO reflections. In addition, at the calcination temperature of 700 °C, the structure of laponite as host material was found to be destroyed. The presence of broader reflection with less intensity at around 30° probably due to the presence of amorphous silica particles as result of structure destruction. The effect is confirmed by DTA-TGA analysis of ZnO dispersed ZnO-SiO_2/LAP sol before calcination (Fig. 4).

The DTA curve of ZnO-SiO_2/LAP shows the intense endothermic peak related to water loss (30-110 °C) followed by weight loss as indication of dehydration process during thermal treatment. Further endothermic effect occured at around 250-700 °C and small peaks at 475, 525, 610 and 625 °C. Compared to the DTA-TGA thermogram of laponite is smoother in the same range and peaks that are not correlated with weight loss expressed the presence of phase change of either SiO_2 or ZnO.

Effect of ZnO-SiO_2 insertion in laponite matrix to the light absorbancy was measured by diffuse reflectance UV-visible measurement. Spectra obtained is presented in Fig. 5. The absorbance spectra of ZnO-SiO_2/LAP lays between the spectra of ZnO-SiO_2 and laponite. By the Zn content of 5.3 %, the spectra shows the values at little bit lower compared to the

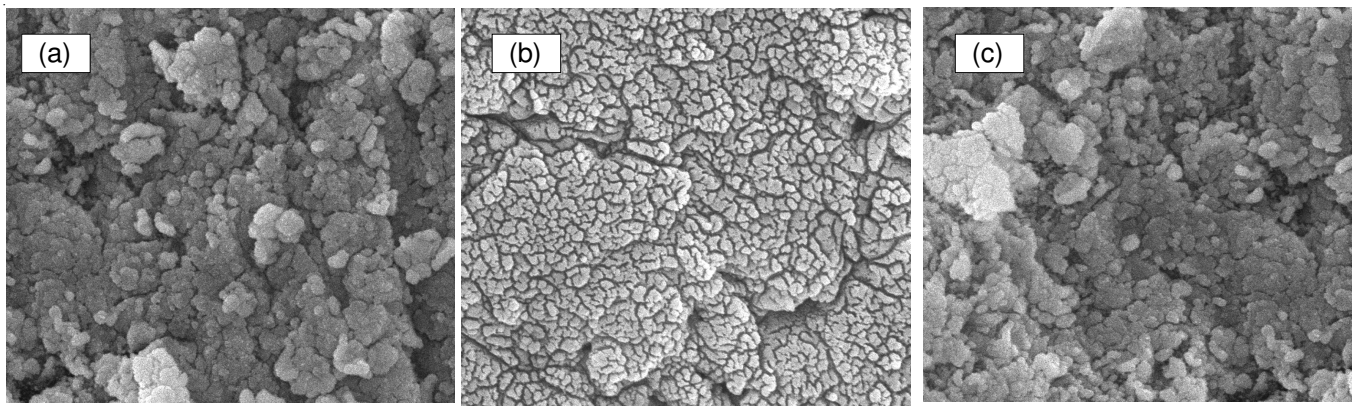

Fig. 3. SEM profile of (a) ZnO-SiO_2 (b) ZnO-SiO_2/LAP-700 (c) ZnO-SiO_2/LAP-600

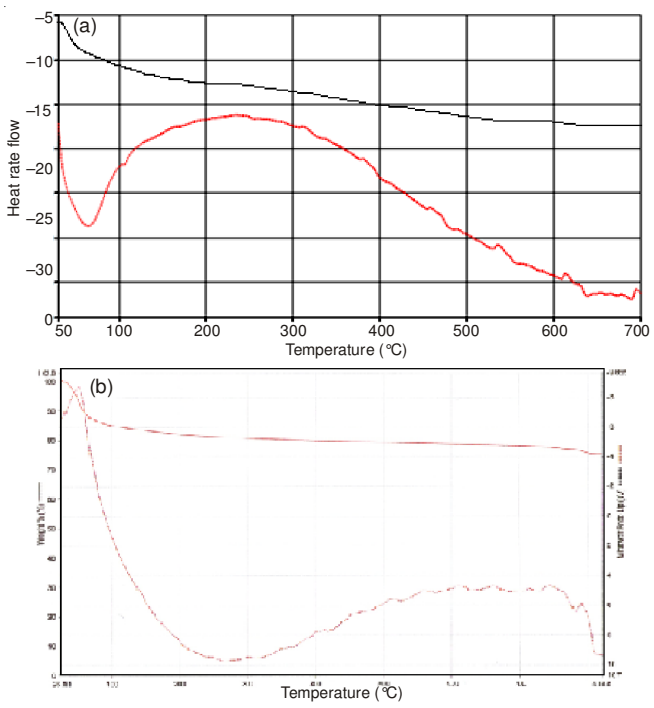

Fig. 4. DTA-TGA curve of (a) ZnO-SiO_2 (b) ZnO-SiO_2/LAP-600

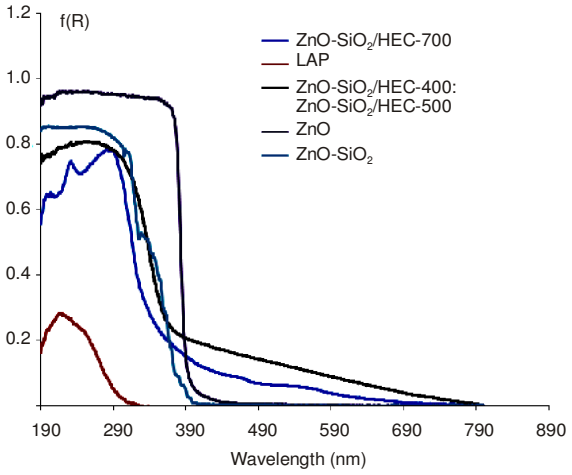

Fig. 5. Spectra obtained from diffuse reflectance UV-visible analysis to the ZnO-SiO_2 and ZnO-SiO_2/LAP samples and laponite compared to bulk ZnO

spectra of ZnO-SiO_2 in all varied wavelength. Diffuse reflectance UV-visible spectroscopy was used to confirm the absorbancy of photocatalysts material. All samples showed the edge wavelength of the absorbancy peaks at around 390 nm. Bulk ZnO give the edge wavelength at 392 nm corresponding to its band gap energy of 3.16 eV. After the combination with SiO_2 in the form of ZnO-SiO_2, there was a slightly blue shifted to around 390 nm indicate the nanoparticles formation of ZnO in composite form. Similar pattern were expressed by ZnO-SiO_2/LAP-400 and ZnO-SiO_2/LAP-600 that were coincide each other confirmed that the ZnO-SiO_2 immobilized nanoparticles on hectorite matrices demonstrated the ability to absorb light in similar wavelength range. The spectra also inform that at the range of 400-600 °C, calcination temperature does not affect the bad gap energy. Furthermore, the different pattern shown by ZnO-SiO_2/LAP-700 in that there is decreasing

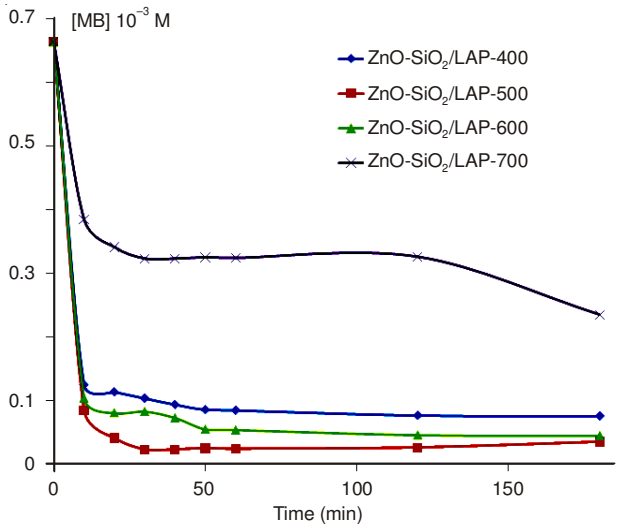

Fig. 6. Kinetics of methylene blue decolorization over ZnO-SiO_2/LAP from varied calcination temperatures

absorbance in all wavelength range pobably relatd to the change of material structure from thermal effect as confirmed by XRD pattern as well as surface area analysis.

Furthermore, photocatalytic activity of prepared material in methylene blue decolorization was evaluated. Photoactivity of ZnO-SiO_2/LAP materials with varied calcination temperature was then tested in methylene blue photooxidation. Kinetics of methylene blue photooxidation depicted in Fig. 6 suggested that the highest photoactivity is obtained by ZnO-SiO_2/HEC-600 while the lowest is ZnO-SiO_2/HEC-700. The results seems to be fit with the specific surface area, XRD and diffuse reflectance UV-visible data in that in general the photocatalytic mechanism is driven by adsorption mechanism[3].

To evaluate effect of ZnO-SiO_2 immobilization in Laponite support, Fig. 7 presents the comparison of methylene blue decolorisation under adsorption, photolysis, photocatalysis and photooxidation treatment over ZnO-SiO_2/LAP-600 and ZnO-SiO_2.

Kinetic curves display the increased methylene blue decolorization by the present of ZnO-SiO_2 and ZnO-SiO_2/LAP photocatalyst. methylene blue decolorization does not occurs by photolysis as indicated by a relative constant concentration at varied treatment time. By adsorption treatment, the kinetic curve of methylene blue decolorization was increased related to the role of porous structure of materials. Furthermore rapid decrease of methylene blue concentration achieved by photocatalysis and photooxidation compared to photolysis which explain that photocatalyst contribute to supply radicals for methylene blue degradation by its catch in photon from UV lamp as light source. It is also strengthened by higher rate of photooxidation over photocatalysis in that the more radicals produced and available in the photooxidation system by H_2O_2 addition as oxidant. By comparing the kinetic curves of photocatalysis and photooxidation by ZnO-SiO_2 and ZnO-SiO_2/LAP-600 photocatalyst, it is concluded that the decolorization rate over ZnO-SiO_2/LAP is higher compared to ZnO-SiO_2 which is in line with the kinetic of the adsorption. This data is related to the specific surface area and pore volume as well as the diffuse reflectance UV-visible analysis indicating that ZnO-

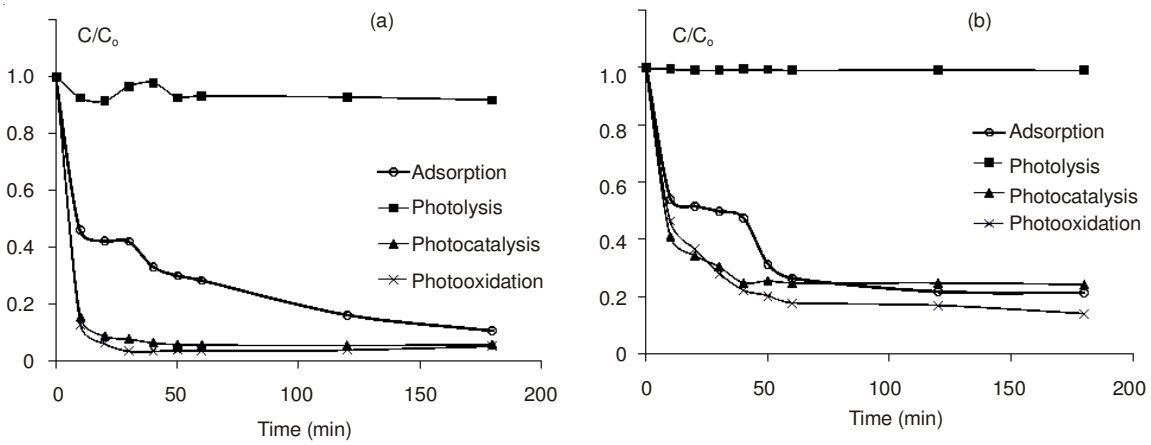

Fig. 7. Comparison on methylene bue (MB) decolorization by varied treatement over (a) ZnO-SiO_2/LAP-600 and (b) ZnO-SiO_2

SiO_2/LAP material has more potency to adsorb methylene blue molecule. Interaction between adsorbed methylene blue on surface and ability of photocatalyst to catch photon play role to enhance methylene blue decolorization. To ensure that methylene blue was delororize with the degradation way is proved by HPLC analysis to the treated solutions (Fig. 8).

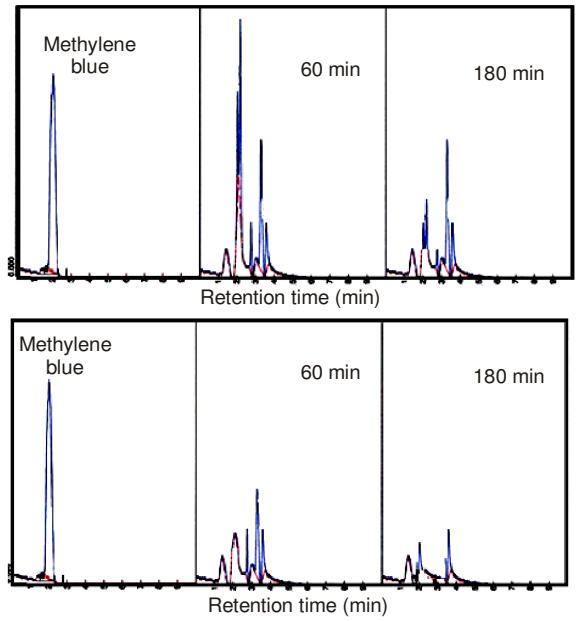

Fig. 8. HPLC analysis of treated solution at varied time over ZnO-SiO_2/LAP-600 (below) and ZnO-SiO_2 (above)

Degradation products are identified from other peaks appeared in treated solution (60 and 180 min) over both ZnO-SiO_2 and ZnO-SiO_2/LAP-600. Effect of the degradation is also presented by COD analysis which the curve is displayed in Fig. 9. Degradation of methylene blue is in line with COD reduction in all varied treatments representing the lower oxidation state of molecules in the treated solution.

Conclusion

The photocatalytic degradation of methylene blue can be conducted by using prepared ZnO-SiO_2/LAP nanoparticles

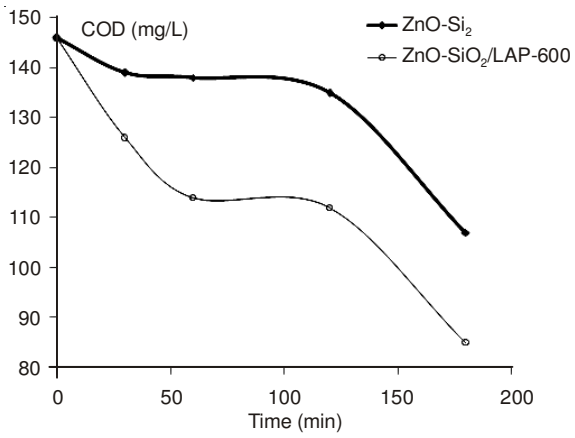

Fig. 9. COD reduction in photooxidation treatment by ZnO-SiO_2 and ZnO-SiO_2/LAP-600

under UV light. The degree of degradation of methylene blue was obviously related to the physicochemical character of material and was affected by calcination temperature.

REFERENCES

1. T. Xu, L. Zhang, H. Cheng and Y. Zhu, *Appl. Catal. B*, **101**, 382 (2011).
2. Y. Li, W. Xie, X. Hu, G. Shen, X. Zhou, Y. Xiang, X. Zhao and P. Fang, *Langmuir*, **26**, 591 (2010).
3. N. Daneshvar, S. Aber, M.S. Seyed Dorraji, A.R. Khataee and M.H. Rasoulifard, *Sep. Purif. Technol*., **58**, 91 (2007).
4. M. Qamar and M. Muneer, *Desalination*, **249**, 535 (2009).
5. M.A. Behnajady, N. Modirshahla and R. Hamzavi, *J. Hazard. Mater*., **133**, 226 (2006).
6. R.M. Mohamed, E.S. Baeissa, I.A. Mkhalid and M.A. Al-Rayyani, *Appl. Nanosci*., **3**, 57 (2013).
7. R.M. Mohamed, I.A. Mkhalid, E.S. Baeissa and M.A. Al-Rayyani, *J. Nanotechnol.*, Article ID 329082 (2012).
8. K.-S. Kim, H.W. Kim and C.M. Lee, *Mater. Sci. Eng*., **98**, 135 (2003).
9. M. Abdullah, S. Shibamoto and K. Okuyama, *Opt. Mater.*, **26**, 95 (2004).
10. J. Zhai, X. Tao, Y. Pu, X.-F. Zeng and J.-F. Chen, *Appl. Surf. Sci*., **257**, 393 (2010).